The proto-oncoprotein SYT (SS18) controls ATP release and regulates cyst formation by polarized MDCK cells

Manesh Chittezhath[*], **Andrea L Frump**[*], **Jerome Jourquin**[*], **Nichole Lobdell**[*], and **Josiane E Eid**[*]

[*] *Department of Cancer Biology, Vanderbilt University Medical Center, Nashville, TN 37232*

Abstract

The SYT proto-oncoprotein (also known as SS18) is a gene expression regulator conserved across species. Although its biological function is still unknown, the importance of SYT as a housekeeping protein is illustrated by the lethal phenotype of SYT-null embryos. Notably, SYT is a component of the synovial sarcoma-associated translocation product, the SYT-SSX oncogene. SYT was previously reported as a mediator of cell adhesion. In the present study we show that SYT possesses distinct domains that control MDCK cyst formation in three-dimensional collagen cultures. While the carboxy-half of SYT, the QPGY domain, is required for cyst growth, the amino-terminal region appears to exert on this process a regulatory effect. Further analysis suggested that the purinergic G protein-coupled P2Y receptor signaling is involved in SYT-induced cystogenesis. Activation of this cascade is due to facilitation of ATP release in the extracellular space of polarized MDCK cells by SYT. These studies allow us to begin to understand the vital role of SYT in controlling epithelial morphogenesis and might explain the lethality of its loss in the developing embryo.

Keywords

SYT; SS18; MDCK; Cystogenesis; ATP

INTRODUCTION

The *SYT* (SYnovial sarcoma Translocated) proto-oncogene is involved in the unique translocation event t(X;18)(p11.2;q11.2) that occurs in synovial sarcoma, a soft tissue tumor. During the chromosomal rearrangement, the *SYT* gene on chromosome 18 is fused to an *SSX* gene, on the X chromosome. This results in the formation of the SYT-SSX chimera in which the C-terminal region coding for the last eight amino acids of SYT is replaced by the C-terminal half of SSX [1,2]. The *SYT-SSX* oncogene is detected in over 90% of synovial sarcomas cases and is implicated in the development of the tumor. Interestingly, it is generally believed that the normal function of SYT is altered in synovial sarcomas, in part due to SYT-SSX formation on one allele, and in part to downregulated expression of the remaining *SYT* wild type allele. Despite the apparent loss if intact SYT in synovial sarcoma, it remains to be seen whether loss of its proper function contributes to tumor development [3,4].

The *SYT* gene is well conserved during evolution. Ubiquitous SYT expression was identified in the early stages of mouse embryonic development whereas in later stages SYT expression is confined mainly to cartilaginous, neuronal and epithelial tissues [5,4]. Targeted knockout of the murine *SYT* gene resulted in a recessive embryonic lethal phenotype due to placental failure, indicating that SYT is essential in early development [6]. Although the protein is localized in the nucleus in specific speckles, it has no recognizable nucleic acid-binding motifs and its biological function is still unclear. SYT has two recognized functional domains, a conserved N-terminal homology domain (SNH; amino acids 15–73), and a region rich in glutamine (Q), proline (P), glycine (G), and tyrosine (Y), called the QPGY domain (resembling the composition of a number of transcription activators). The QPGY domain constitutes the C-terminal half of SYT (amino acids 187–387) [7] and was shown to activate gene transcription in an *in vitro* system [7,8] as well as synergize with nuclear receptors to activate gene expression *in vivo* [9,10]. The SNH domain appears to interact directly with the acute leukemia-associated transcription factor AF10 [11], the human homologues SWI/SNF ATPases BRM and BRG1 [7,12], the histone acetyltransferase p300 [13] and the co-repressor mSin3A [14]. It was also reported that in contact inhibited cells, p300 but not CBP binds to the N-terminal region of SYT and forms a complex in the nucleus of G1-arrested cells. This nuclear SYT/p300 complex appeared to regulate cell adhesion, a function that is lost when a part of SYT-C-terminal region is deleted [13]. *In vitro* studies showed that deletion of the SNH domain enhanced the transcriptional activation potential of SYT, suggesting that this domain regulates QPGY-driven activation. The QPGY-mediated transcriptional activation capacity and the lack of obvious DNA-binding domains, suggest that the SYT functions in gene expression regulation by protein-protein interactions [6].

Three-dimensional (3D) cultures of epithelial cells grown in thick gels of extracellular matrix material (ECM) such as type-1 collagen or Matrigel® represent a very useful system to study cellular and molecular mechanisms underlying epithelial morphogenesis. Mardin–Darby canine kidney (MDCK) cells, an epithelial cell line derived from the distal tubules of canine kidney, when cultured in Type-1 collagen gel as a single cell suspension, undergo proliferation, growth arrested differentiation and produce mainly clonal cysts comprised of a monolayer of polarized epithelial cells enclosing a fluid filled central lumen. In these cysts, the apical surface of the polarized monolayer faces the central lumen and the basolateral surface is in contact with the ECM and neighboring cells [15,16]. Epithelial cyst formation and enlargement are the result of a highly coordinated signaling network involving cell proliferation, fluid accumulation within the cyst cavity and extracellular matrix remodeling [17,18]. The development and maintenance of these polarized structures is a fundamental feature in the biology of epithelial cells and disruption of this intact, well-ordered architecture forms the basis of epithelial tumors or carcinomas [19]. Moreover, epithelial cystogenesis contributes to various physiological and pathological processes and its deregulation is the basis of polycystic kidney disease pathogenesis. One advantage of 3D epithelial culture systems is that they recapitulate some of the essential structural features of glandular epithelium *in vivo*. They also provide an accessible system to identify the signaling events responsible for the formation and maintenance of 3D epithelial structures [20].

One of the major mediators involved in cystogenesis signaling is extracellular ATP. Secreted ATP in the lumen functions as a ligand for the purigenic G-protein coupled P2Y receptors. Once activated, these receptors can cause intracellular Ca^{2+} mobilization or increased Cl^- ion transport into the lumen of the epithelial cysts that can osmotically drive fluid movement and increase cyst size. MDCK cells are known to possess an ATP stimulated Cl^- ion secretory mechanism [21] and they also express different P2Y receptors [22]. It has also been shown that stimulation of endogenous P2Y receptors by extracellular ATP increases the growth of MDCK cyst [23]. ATP released by the cells lining the cyst lumen is trapped inside and creates an autocrine/paracrine loop of nucleotide signaling and thus plays an important role in epithelial

cyst volume regulation [24]. In the present study and for the first time, we explored the role of SYT in maintaining tissue integrity during epithelial cell morphogenesis in a 3D context using the collagen-MDCK cells as a model system. We show that the N-terminal region of SYT exerts a regulatory role on cystogenesis while the carboxy-half of SYT is needed for cyst formation. This regulation may occur, at least in part, through secretion of ATP in the extracellular space.

MATERIALS AND METHODS

Cell lines, lysis, antibodies and reagents

MDCK cells were obtained from ATCC (Manassas, VA) and cultured in 5% CO_2 at 37°C in Dulbecco's minimal essential medium (DMEM) (Invitrogen, San Diego, CA) containing 10% fetal bovine serum. For cell lysis, equal number of cells were pelleted and lysed by adding an equal volume of 2X SDS-PAGE sample buffer followed by boiling. For immunoblots and immunofluorescence studies, anti-hemagglutinin (HA; Sigma, St. Louis, MO), Phalloidin conjugated rhodamine, (Actin; Sigma, St. Louis, MO), anti-β catenin, anti-GM-130, anti-pancadherin (BD transduction laboratories, Lexington, KY) anti-ZO-1, anti-Occludin (Zymed laboratories, CA), were used. For inhibition of MDCK cysts, the following compounds were used: Reactive Blue 2 (Alexis Biochemicals, San Diego, CA), PPADS (Sigma, St. Louis, MO), PD98069, AG1478, NF023, LY290042, H-89, Calphostin C, W7, SP-600125, SB-220025, and Rac1 Inhibitor, all from Calbiochem (La Jolla, CA). Concentrations used and treatment times are all mentioned in Table-1 and in the Results section. The ATP Bioluminescent assay kit was purchased from Sigma (St. Louis, MO).

Retroviral constructs and transfection of MDCK cells

Full-length (WT) SYT and SYTdl 8 in the pOZ vector were generated as previously described [25]. For the construction of SYT dl 1–40, the insert was obtained by PCR amplification using full-length SYT as a template with: 5′GCGCCTCGAGTAGACCACCATGACCTCA GAGTGTTCTCAGTATCAGCAG 3′ and 5′ GCGCGCGGCCGCCTGCTGGTAAT TTCCATACTGTCCC 3′ as forward and reverse primer, respectively. The PCR product was then cut with Xho1 and NOT1, inserted in the pOZ vector digested with the same enzymes. The integrity of the pOZ SYTdl 1–40 was confirmed by sequencing. The SYT 1–164 mutant was obtained with a complete NOT1 digestion of WT SYT, followed by a partial digestion with BamH1 and re-annealing of the same vector with the double-stranded adaptor: 5′ GATCCATGGGAGGTTACAACGC 3′ and 5′ GGCCGCGTTG TAACCTCCCATG 3′. The SV-40 NLS was inserted in SYT 1–164 using the Quick Change site directed mutagenesis System by Stratagene. The PCR primers used were forward:5′ CTCGAGTAGACCACCATGCCAAAAAAGAAGAGAAAGGTAGAG TCTGTGGCTTTCGCG 3′ and reverse 5′CGCGAAAGCCACAGACTCTACCTTTCTCTT CTTTTTTGGCATGGTGGTCTACTCGAG 3′. The underlined sequence corresponds to the SV-40 T antigen NLS sequence. Transient retroviral infections were performed using the phoenix packaging cell system, as described previously [25].

3-Dimensional culture of MDCK cells

MDCK cysts were prepared by suspending cells (2.5×10^4/mL) in 8 part ice cold liquid Rat tail type1 collagen (BD biosciences) neutralized with NaOH at a final concentration of 1.8mg/ml and containing one part minimum essential medium (MEM) and one part 1X DMEM. 0.4ml of the collagen suspension is then poured on each well of the 8- well chamber slide. After gelation, 0.4 ml of growth medium was layered over the gel. The cells were grown in 5% CO_2 at 37°C and were fed every 2 days with fresh medium until cysts with lumen were formed.

MDCK cyst number and enlargement; data analysis

Individual cysts derived from the clonal growth of single MDCK cells could be visualized by day 4. The number of cysts in the well and the size of individual cysts were determined on the 8th day. Plates were examined with an inverted microscope (Zeiss, Axiovert 200M). For this study a cyst is defined as a spherical structure with a distinct cell wall and a central lumen. All cysts with a diameter larger than 50μm were counted at 20x magnification. They generally fell in one of the three categories; large: >250 μm diameter, medium: 150–250 μm diameter, small: <150 μm in diameter.

Indirect immunofluorescence

For indirect immunofluorescence studies, cells were fixed in 4% paraformaldehyde, permeabilized in 0.2% Triton X-100 and blocked with 3% goat serum. Coverslips were incubated with primary antibodies for 2 hours and Alexa-conjugated secondary antibodies (Molecular Probes, Eugene, OR) were used. A Zeiss (Axioplan 2) fluorescence microscope (Thornwood, NY) was used for visualization.

Polarization of MDCK cells cultured on Transwell filters

MDCK cells transfected with pOZ plasmids were cultured on 12-mm Transwell filters coated with collagen (0.4 um pore size, Costar) for 4 days. Immunostaining was performed as described above with a few modifications. Cells were fixed in paraformaldehyde for 30 minutes, permeabilized for 10 minutes, and blocked for 1hour in 2%BSA in PBS. Primary antibodies diluted in blocking buffer were then added simultaneously to both apical and basolateral sides and incubated for 2 hours. Cells were washed and incubated with Alexa-conjugated secondary antibodies on both compartments for 45 minutes. The filters were excised for visualization.

Immunofluorescence of MDCK cysts and confocal microscopy

MDCK cysts were allowed to form in collagen 3D gels after growing for 6–7 days. The gels were digested with 200U/ml collagenase (C2399, Sigma) in PBS for 30 minutes at 37°C to partially dissolve collagen. Cysts were fixed in 4% paraformaldehyde (PFA) for 20 minutes at room temperature, permeabilized in 0.5% Triton-100/PBS for 20 minutes, rinsed 3 times with PBS/Glycine and then blocked with 10% goat serum for 45 minutes at room temperature. The samples were incubated with primary antibodies in block solution overnight at 4°C. After extensive washing, the samples were incubated with Alex-flour conjugated secondary antibody for 2 hours at room temperature. All images were obtained using a Zeiss LSM 510 confocal microscope.

Quantitation of ATP production and release from monolayers of polarized MDCK cells

Bioluminescence detection of ATP released from polarized epithelial cells was carried out as previously described [26], with some modifications. Briefly, MDCK cells transfected with pOZ plasmids were seeded at high density (10^5 cells/12-mm filter) on to collagen-coated permeable supports (Millicell, 12mm diameter, permeable filter cups). The epithelial monolayers were grown in medium added to both apical and basolateral sides of the cells (upper and lower chambers of the filter supports respectively) for 2 days. After that initial period, the apical side was devoid of medium, whereas the basolateral side was fed daily. Monolayers were grown in this manner until no fluid leaked from the basolateral space in to the apical side or filter cup, to ensure confluence of the monolayer. Cells were then fed with fresh medium on both sides of the monolayer and incubated overnight. To measure ATP release, monolayers were washed twice with PBS on both sides, and 200 ul of Opti-MEM1 (Invitrogen) medium were added to both chambers and incubated for 30 minutes. 100 ul of the culture medium were taken from both filter cup (apical) and culture plate (basolateral) and added to an equal volume

of ATP assay mix solution (sigma). The chemiluminescent signal was measured with a PharMingen Monolight 3010 luminometer and recorded as Relative Light Units (RLU). To measure cellular ATP production, cells were washed twice with PBS and then lysed with 100 ul of Reporter Lysis buffer (Promega) and rocked for 30 minutes at 4°C. ATP measurement was performed as described above using the ATP Bioluminescent assay kit from Sigma.

Transient siRNA transfection

SiRNA transfections were performed as described previously [27]. The Si-SYT :5′ GUACAGAAUCAGAUGACAAUU3′ oligomer (Dharmacon Research Inc., Chicago, IL) was used for specific SYT depletion. A non-silencing inverted (INV) sequence [25] was used as control. Cells were harvested 24 hours after siRNA treatment and plated on to collagen-coated permeable supports. ATP release was measured 24 hours later as described above.

RESULTS

The SYT QPGY domain is required for normal growth of MDCK cysts

Following previous work that demonstrated a role of SYT in cell adhesion control [13], we aimed to further understand SYT contribution to epithelial structure formation in a three-dimensional (3D) context. When cultured in collagen gels, MDCK cells undergo proliferation, develop as hollow cysts and accumulate fluid within the cyst cavity while remodeling the ECM. We therefore adopted this culture model to explore the role of SYT in the regulation of cyst formation. MDCK cells were transduced with retroviral vectors (pOZ) expressing Wild Type (WT) SYT and various SYT deletion mutants (Fig. 1A). The cells were then allowed to grow in a 3D collagen gel for 7–10 days. All proteins were expressed at high efficiency (80–90% infection rate; Fig. 1D) and at equivalent levels (Fig. 1E). Importantly, stable integration of the retroviral vectors in the transduced cells allowed us to perform these studies over the extended periods required. Starting from day 4, individual cysts derived from clonal growth of MDCK cells could be visualized. We observed that WT SYT stimulated MDCK cells to form larger cysts than with pOZ vector control or untreated cells. It was, however, deletion of the N-terminal 40 amino acids of SYT (SYTdl 1–40) that conferred on MDCK cells the ability to form cysts of a significantly larger volume than all the remaining transfectants (Fig. 1B,C). Deletion of the last eight amino acids (SYTdl 8) did not cause a detectable change in the number and size of the cysts from WT SYT-expressing cells. Interestingly, however, SYT 1–164 NLS-expressing MDCK cells formed no cysts, or if formed, the cysts were very small in size and much fewer in numbers compared to vector control (Fig. 1B,C). SYT 1–164 comprises the amino-terminal half of SYT fused to a nuclear localization signal (NLS; see materials and methods). NLS was added to target SYT 1–164 to the nucleus and enable comparison of its effect on cyst formation with that of WT SYT and the remaining mutants, all nuclear proteins. Exogenously expressed SYT 1–164 lacking the NLS yielded results identical to SYT 1–164 NLS effects in inhibiting cyst formation (data not shown). The distribution of SYT 1–164 protein, however, was pancellular (data not shown) and necessitated the incorporation of a standard NLS sequence to concentrate it in the nucleus.

Altogether, these results suggest that the proto-oncoprotein SYT contains distinct functional domains that actively regulate cyst formation by MDCK cells. While expression of WT SYT potentiated MDCK cysts growth, the QPGY domain (absent in SYT 1–164) was required for their formation. Conversely, the N-terminal region of SYT containing the first 40 amino acids appeared to exert a regulatory role on the morphogenesis of the MDCK 3D-cultures.

The SYT QPGY domain controls MDCK signaling in a 3-D context

The inability of MDCK cells expressing SYT 1–164 to form cysts led to the question whether this phenotype was a consequence of a defect in cellular growth or adhesion, or both. To address

this question, we performed standard assays on MDCK cells growing in monolayers. When compared to naive cells or vector control, MDCK cells expressing WT SYT, SYTdl 8, SYTdl 1–40 and SYT 1–164NLS exhibited no change in their growth and proliferation rate in the presence of high (10%) or low (0.2%) serum. There was no evidence of accelerated apoptosis and we detected no difference in their ability to adhere and spread on collagen. Moreover, SYT 1–164 and SYTdl 1–40 cells showed no difference in migration on collagen-coated filters or invasion in collagen matrices. Finally, when tested in cell-cell adhesion assays, SYT 1–164 and SYTdl 1–40 cells could aggregate at a rate equivalent to that of WT SYT and the remaining SYT mutant expressants (data not shown). We also failed to detect a differential distribution of polarity and adhesion markers (ZO-1, β-catenin, GM 130, F-actin and cytoskeletal tubulin) between MDCK cells expressing the vector, WT SYT and all the SYTdl mutants (data not shown). Consistent with the immunostaining results, western blot analysis of lysates derived from cells expressing WT SYT, SYT 1–164 and SYTdll1–40 revealed no change in the levels of polarity marker proteins (Fig. 2B). The normal growth and adhesion behavior of MDCK cells in the two-dimensional context of monolayers suggested that SYT 1–164- and SYTdl 1–40- induced phenotypes are likely due to disruption of the signaling network governing the integrity of the cyst in the context of 3D collagen gels. Characterizing the SYT 1–164 NLS phenotype will therefore necessitate studies on the 3D culture systems with tissue-like organization and specified polarity.

First we wanted to confirm that the enlarged SYTdl 1–40 expressing MDCK cyst is not the result of increased cell proliferation. We thus stained the cysts with Ki-67 and an antibody to activated caspase-3 and found no evidence for increased proliferation or apoptosis (data not shown). This led to the conclusion that enlargement of SYTdl 1–40 cysts is due to an increase in fluid accumulation within the cavity resulting in lumen expansion [28] and a flattened appearance of the cells (Fig. 2A). Since cell polarity plays a crucial role in regulating tissue integrity during epithelial morphogenesis we next asked whether the phenotypes induced by SYTdl 1–40 and SYT 1–164 were caused by disruption of the MDCK cell polarity. MDCK cell lines expressing WT SYT, the various SYT mutants or vector alone were cultured in 3D collagen Type1 matrix up to 7 days and immunostained with polarity markers. In this culture system, control cells formed a single polarized monolayer enclosing a centrally placed lumen. In control cysts, confocal microscopy showed that F-actin was mainly localized at the apical surface surrounding the lumen, whereas β-catenin was localized at the basolateral surface (Fig. 2A). ZO-1 was seen at the tip of the cell-cell junctions towards the apical surface (Fig. 2A). In polarized epithelial cells, the Golgi is localized in between the nucleus and the apical surface of the cell as seen by staining with GM-130 (Fig. 2A). Expression of WT SYT and the various SYT mutants was confirmed by staining with anti-HA antibody (Fig. 2A). Except for MDCK cells expressing SYT 1–164NLS which formed rudimentary cysts and no lumen, WT SYT, SYTdl 8 and SYTdl 1–40, all formed cysts with normal polarity and a central lumen similar to controls. Notably, cysts expressing SYTdl 1–40 were significantly increased in size and the cells were much flatter than those in the controls, but the polarity markers were properly localized at their appropriate locations. Taken altogether, these data suggest that the SYT proto-oncoprotein mediates normal MDCK cyst formation through its carboxy-terminal half or QPGY domain (aa 165–387). For this function, SYT responds to the intricate signaling network that integrates multiple events involved in the formation of 3D structures. Such signaling network is not active in non-polarized 2D monolayer cultures and this explains the normal behavior of SYT1-164NLS cells when grown as monolayers.

Effect of P2Y receptor cascade inhibitors on the growth and morphology of MDCK cysts

Our studies so far imply that WT SYT expression promotes cyst formation by MDCK cells. Moreover, the removal of the N-terminal region (SYTdl 1–40) alleviates a regulatory effect and stimulates formation of even larger cysts. We were next interested in determining whether

WT SYT and SYTdl 1–40 exert their stimulatory effect as part of the 3D signaling network known to control MDCK cystogenesis. We started by inhibiting the signaling mediators of this network (Fig. 6; diagram) and assessing their effect on cyst growth. WT SYT- and SYTdl 1–40- expressing MDCK cells were grown in collagen gels for 8 days. Inhibitors of key signaling effectors were added twice to the cysts, on the fourth and the sixth day of collagen culture. Inhibition of MEK1, (PD98069), JNK (SP600125), p38 MAPK (SB220025) as well as the general inhibition of tyrosine kinase activity (genestein) and Rac1 completely abolished the growth of both WT SYT as well as SYTdl 1–40 expressing cysts (Table-1). PI3 Kinase inhibition (LY290043) resulted in partial reduction in the growth of both WT SYT as well as SYTdl 1–40 cysts when compared to cysts derived from naïve or pOZ- transduced MDCK cells. It was previously reported that MDCK cells express P2Y receptors, a family of purinergic G protein-coupled receptors (GPCR) known to play an essential role in the biology of cyst formation [23]. To assess the involvement of the P2Y receptors in SYT- and SYTdl 40- cyst promotion, we treated MDCK cells expressing these two proteins with two potent P2Y-specific inhibitors [23], reactive blue 2 (RB 2) and pyridoxal-phosphate-6-azophenyl-2′, 4′-disulfonate (PPADS). At 500 uM, RB 2 caused a complete arrest of cyst growth by SYT- and SYTdl 1–40 expressants. An equal concentration of PPADS, a less effective but still potent P2Y inhibitor, induced a profound reduction in intact cysts (Tables 1,2 and Fig. 3). Conversely, inhibition of the P2X receptor- an ATP-gated cation channel known to mediate epithelial cell function - with NF023 had no effect on the growth of MDCK cysts, suggesting no involvement of P2X receptors in this process.

In summary, the effect of the various signaling inhibitors suggests that modulation of MDCK cyst growth by SYT involves key mediators known to function in the canonical signaling network of cyst/lumen formation, controlled by the P2Y receptors. The similar sensitivity of WT SYT- and SYTdl 1–40-expressing cysts to inhibition by P2Y antagonists is expected since both proteins contain an intact QPGY domain. The inhibition data also suggest that the N-terminal deletion in SYTdl1–40, though it confers additional cyst growth, does not abolish regulation by the P2Y cascade inhibitors.

SYT controls apical and basolateral ATP release by polarized MDCK cells

Our data so far show that specific domains of SYT play an important role in MDCK cyst formation. They also imply that P2Y receptor signaling may actively participate in this process. To further understand the regulation of cystogenesis by SYT, we decided to identify the level at which the proto-oncoprotein might influence P2Y signaling. P2Y receptors are normally activated by nucleotide agonists that include ATP or UTP. When MDCK cysts form, the polarized epithelial cells release ATP in the luminal space. Through P2Y activation, secreted ATP regulates epithelial Cl^- and Na^+ channels, fluid secretion, and cell volume by autocrine and paracrine mechanisms. To start understanding the role of SYT in this process, we inquired whether SYT is involved in the control of ATP release by the polarized MDCK cells. Since the microscopic scale of MDCK cysts does not allow accurate measurement of luminal ATP secretion, we decided to perform these assays on MDCK cells grown and polarized on flat collagen-coated filters. Cells expressing WT SYT and SYT dl mutants were thus grown (1×10^5/well) as polarized monolayers on collagen filters (Fig. 4A). After reaching confluence, ATP release from their apical as well as basolateral membranes was measured using a bioluminescence-based method. In this assay, we observed that ATP secreted by MDCK cells occurred largely across the apical membrane. We also observed that the level of ATP secreted by SYT 1-164NLS-expressing cells on their apical side was significantly reduced compared to vector control. Basolateral ATP secretion was also reduced in cells expressing SYT 1–164 but to a lesser extent than the apical ATP release. Notably, both apical and basolateral ATP secretion were significantly enhanced in MDCK cells expressing SYTdl 1–40 compared to vector control and the remaining SYTdl mutants. The levels of extracellular ATP in the medium

of WT SYT cells was also higher than in vector control but to a lesser extent than in SYTdl 1–40 media (Fig. 4A,B).

These results correlate the ability of polarized MDCK cells to secrete ATP with their capacity to form cysts in collagen gels. SYTdl 1–40 cells form lumens with the largest volume and release the highest concentration of ATP in the extracellular medium, while SYT 1–164NLS cells lack the ability to both form intact cysts and release an adequate amount of ATP. It appears from these data that the same SYT domains regulate both functions. Based on the existing knowledge that extracellular ATP is a potent agonist for cystogenesis through P2Y receptor stimulation, it is reasonable to assume that SYT regulates cyst formation by controlling ATP release from polarized cells lining the cyst.

To determine whether these changes in ATP release are due to a genuine effect of SYT on ATP secretion signaling or they merely reflect differences in ATP synthesis, we measured intracellular ATP levels in the various groups of polarized MDCK infectants. In these assays, contrary to their unequal rate of ATP release in the extracellular medium, WT SYT and the SYT mutants appeared to contain equivalent steady state levels of total ATP (Fig. 4C). These data suggest that SYT contributes to the control of ATP release from the polarized cell and does not affect intracellular ATP production.

To further confirm that SYT is involved in the control of ATP secretion by polarized MDCK cells, we specifically depleted SYT in MDCK cells by RNA interference (Si-SYT). 24 hours after transfection, MDCK cells were plated at high density (1×10^5/well) on collagen- coated filters and ATP released by the polarized cells at the apical and the basolateral was measured 24 hours later (optimal time for SYT depletion; Fig. 5B). When compared to cells transfected with an inverted (INV) control RNA duplex, MDCK cells depleted of almost ninety percent of their endogenous SYT released ATP at markedly reduced levels. This effect was more profound on the apical surface (Fig. 5A).

Taken altogether, our results implicate SYT in the control of MDCK cyst formation. This regulation is exerted by distinct N-terminal and C-terminal domains of SYT. Our finding that cellular SYT affects ATP release by the polarized epithelial cells suggests that modulation of cystogenesis by SYT is mediated, at least in part, by ATP/P2Y signaling.

DISCUSSION

In this report we present findings concerning the cellular function of the SYT proto-oncoprotein. The studies follow the initial observation that SYT forms a nuclear, G1-specific complex with p300, a histone acetyl transferase and a transcription co-activator, and this SYT/p300 complex is actively involved in the regulation of cell adhesion. While p300 and other chromatin remodeling complexes interact with the N-terminal regions of SYT including the SNH domain, cell adhesion control appeared to be mediated by its C-terminal domains [13]. With this in mind, we decided to extend the analysis of SYT function to 3D-systems that are physiologically closer to tissue morphogenesis. In the present study we used the MDCK-collagen system as a 3D model to study the role of SYT in maintaining tissue integrity. In a collagen gel matrix, single MDCK cells proliferate and differentiate to form multicellular, highly polarized, fluid-filled cysts. The architecture of these cysts recapitulates that of epithelial cell-lined organs and their intricate signaling [29]. Epithelial morphogenesis is a tightly regulated phenomenon that involves cell-cell adhesion, cell-matrix interactions and cell polarization.

In the present study, we found that the proto-oncoprotein SYT regulates MDCK cyst formation through its distinct domains (SNH and QPGY). SYT lacking the QPGY domain (SYT 1–164NLS) allowed a few rudimentary cysts to form at best while SYTdl 1–40 which has lost

half of the SNH domain formed very large cysts in significantly high numbers. These results indicate that the SYT-QPGY domain is important for the formation of 3D structures and the N-terminal region of SYT exerts a regulatory effect on epithelial cyst morphogenesis.

Intriguingly, the defective phenotype of SYT 1–164NLS did not translate into any apparent abnormal growth or adhesion when the cells were grown in 2D monolayers. This indicates that this particular function of SYT requires and involves the signaling network integrated in the growth of 3D structures. When tested in monolayers, we detected no change in the levels of key polarity markers such as ZO-1, cadherin, β-catenin, or GM-130 in the cells expressing SYT 1–164NLS or SYT dl 1–40. Moreover, confocal microscopy of cysts derived from the various mutants, including the rudimentary structures without lumen of SYT 1–164NLS, demonstrated a normal distribution of the same markers on polarized cells. Confocal imaging did reveal however what appeared to be an enlarged volume of accumulated fluid in the lumen and a flattened shape of the surrounding polarized monolayer in the SYTdl 1–40-derived cysts. This phenotype prompted the thinking that the N-terminal region of SYT may regulate the signal (s) for fluid accumulation within the cyst.

Our next quest was to begin to understand the biochemical mechanism by which SYT stimulates MDCK cystogenesis. P2Y receptors are GPCRs mainly activated by ATP, ADP and UTP agonists [30]. They belong to a family of eight members and induce divergent signaling pathways (phospholipase C, Rac, adenylate cyclase, RhoA), depending on the heterotrimeric G proteins they activate [31]. In addition to their immediate effectors, the P2Y receptors interact with and regulate a variety of signaling molecules such as ion channels, integrins and growth factor receptors, thereby integrating an intricate signaling network and several biological processes in the polarized cell. MDCK cells express several P2Y receptor subtypes and use multiple signaling pathways for both direct and feedback regulation. Such pathways confer on released nucleotides, in particular ATP, a key role in establishing signaling systems in MDCK cells as well as in other cell types [32]. Once activated by the purine nucleotide, P2Y receptor signaling may lead to phosphoinositide hydrolysis, MAP kinase activation, cAMP production and ERK stimulation via interacting receptor tyrosine kinases. Altogether, these potent signals will exert a mitogenic effect on the epithelial cells and allow them to proliferate and organize into a polarized layer with their apical surface facing a fluid-filled lumen [15,23]. Several of these P2Y pathways can increase ion transport as well and lead to fluid accumulation, by osmosis, in the cyst lumen. Moreover, MDCK cells possess a Cl^- ion secretory mechanism driven by ATP [33].

The definite increase in number and lumen size WT SYT confers on MDCK cysts indicates that the proto-oncoprotein induces positive modulators of the cystogenesis signaling cascade. Deletion of the N-terminal region of SYT eliminated a regulatory domain and led to, if not enhanced proliferation of polarized cells, an increase in the volume of the lumen that resulted in a flattened surrounding monolayer. Increase in luminal fluid by secreted anions is considered the end process of an active signaling network initiated by ATP stimulation of the P2Y purinergic receptors [31]. Inhibition of several members of this network abrogated SYT-promoted cystogenesis (Fig.6). Moreover, inhibition of WT-SYT- and SYTdl 1–40- cysts by PPADS, a potent functional inhibitor of P2 receptors and Reactive Blue 2 (RB2), a potent P2Y receptor blocker [23], suggested that SYT-enhanced cystogenesis likely relies on P2Y signaling. Finally, The drastic decrease in ATP release from the surface of SYT1-164NLS cells (with absent QPGY domain) that are incapable of forming cysts provided a functional link between activation of the ATP-driven cystogenesis cascade and an intact SYT-QPGY domain. The enhanced ATP release by polarized SYT 1-164 cells may therefore explain the increased fluid accumulation and expansion of their cyst lumen.

The role of SYT on ATP release by polarized MDCK cells was further supported by the RNA interference experiments where depletion of SYT resulted in a significant reduction in apical and basolateral ATP release. So far we have been unsuccessful in depleting SYT from MDCK cell lines in a stable fashion. In the transient siRNA assays, SYT levels reverted to normal on the fourth day and we were therefore unable to study SYT-depleted MDCK cells in the 3-D cultures that needed 7–10 days for cyst formation. Combined with the embryonic lethality of SYT-null mice, our data on the effect of SYT on cellular ATP indicate that SYT is a vital protein and the cells are unable to survive without it. This may justify our failure in generating cells with permanent SYT-loss of function.

Altogether the above data clearly indicate a significant role of SYT in MDCK cyst formation. They also suggest that SYT regulates MDCK cyst by controlling the release of ATP from the polarized cells and subsequent activation of the P2Y receptors.

The mechanism of ATP regulation by SYT remains to be discovered. However, given the prevalent function of SYT, it could be surmised that this control occurs at the level of gene expression (Fig. 6), and that it is mediated by the QPGY domain. Conversely, inhibition of ATP release and cyst formation by SYT 1–164 NLS indicates that this mutant exerts a dominant-negative effect on WT SYT. This likely occurs as a consequence of SYT 1–164 sequestering away necessary factors required for QPGY-mediated transcription.

Nucleotides like ATP are ubiquitous extracellular signaling molecules that induce a wide spectrum of biological effects. In recent years considerable efforts have been made in the area of nucleotide signaling to understand their release mechanism in the extracellular fluids, their degradation by ectoenzymes, and the receptors mediating their cellular effects [34]. Altered ATP release and signaling has also been shown to be detrimental to the pathogenesis of autosomal dominant polycystic kidney disease (ADPKD). Elevated ATP release in the lumen of the kidney cysts elicits an autocrine and/or paracrine activation of P2 receptors that ultimately leads to Cl^- and fluid accumulation and volume expansion in ADPKD cysts [24, 35].

The exciting and novel observation of SYT involvement in the regulation of a fundamental metabolic molecule such as ATP has significant ramifications that will help understand essential metabolic processes. It also provides one likely mechanism for failure of proper organ formation during embryogenesis in SYT knock-out mice. SYT is essentially a gene regulator involved in chromatin remodeling and transcription. We can surmise that its apparent effect on ATP release is the consequence of a positive feedback modulator whose expression is induced by nuclear SYT and either directly or indirectly stimulates ATP release machineries (Fig. 6). Extensive molecular characterization is needed to dissect this event and identify the intermediate effectors of this pathway. Such characterization promises to uncover key events in cellular metabolism.

Acknowledgements

References

1. Clark J, Rocques PJ, Crew AJ, Gill S, Shipley J, Chan AM, Gusterson BA, Cooper CS. Identification of novel genes, SYT and SSX. involved in the t(X;18)(p11.2;q11.2) translocation found in human synovial sarcoma. Nat Genet 1994;7:502–508. [PubMed: 7951320]

2. de Leeuw B, Balemans M, Olde Weghuis D, Geurts van Kessel A. Identification of two alternative fusion genes, SYT-SSX1 and SYT-SSX2. in t(X; 18) (p11.2; q11.2)-positive synovial sarcomas. Hum Mol Genet 1995;4:1097–1099. [PubMed: 7655467]

3. Brodin B, Haslam K, Yang K, Bartolazzi A, Xie Y, Starborg M, Lundeberg J, Larsson O. Cloning and characterization of spliced fusion transcript variants of synovial sarcoma: SYT/SSX4, SYT/SSX4v, and SYT/SSX2v. Possible regulatory role of the fusion gene product in wild type SYT expression. Gene 2001;268:73–182.

4. de Bruijn DR, Kater-Baats E, Eleveld M, Merkx G, Geurts van Kessel A. Mapping and characterization of the mouse and human SS18 genes, two human SS18-like genes and a mouse Ss18 pseudogene. Cytogenet Cell Genet 2001;92:310–319. [PubMed: 11435705]

5. de Bruijn DR, Baats E, Zechner U, de Leeuw B, Balemans M, Olde Weghuis D, Hirning-Folz U, Geurts van Kessel A. Isolation and characterization of the mouse homolog of SYT, a gene implicated in the development of human synovial sarcomas. Oncogene 1996;13:643–648. [PubMed: 8760306]

6. de Bruijn DRH, Peters WJM, Chuva de Sousa Lopes SM, van Dijk AHA, Willemse MP, Pfundt R, de Boer P, Geurts van Kessel A. Targeted disruption of the synovial sarcoma-associated *SS18* gene causes early embryonic lethality and affects *PPARBP* expression. Hum Mol Genet 2006;15:2936–2944. [PubMed: 16926188]

7. Thaete C, Brett D, Monaghan P, Whitehouse S, Rennie G, Rayner E, Cooper CS, Goodwin G. Functional domains of the SYT and SYT-SSX synovial sarcoma translocation proteins and co-localization with the SNF protein BRM in the nucleus. Hum Mol Genet 1999;8:585–591. [PubMed: 10072425]

8. Brett D, Whitehouse S, Antonson P, Shipley J, Cooper C, Goodwin G. The SYT protein involved in the t(X;18) synovial sarcoma translocation is a transcriptional activator localised in nuclear bodies. Hum Mol Genet 1997;6:1559–1564. [PubMed: 9285794]

9. Iwasaki T, Koibuchi N, Chin WW. Synovial sarcoma translocation (SYT) encodes a nuclear receptor coactivator. Endocrinology 2005;146:3892–3899. [PubMed: 15919756]

10. Perani M, Antonson P, Hamoudi R, Ingram CJ, Cooper CS, Garrett MD, Goodwin GH. The proto-oncoprotein SYT interacts with SYT-interacting protein/co-activator activator (SIP/CoAA), a human nuclear receptor co-activator with similarity to EWS and TLS/FUS family of proteins. J Biol Chem 2005;280:42863–42876. [PubMed: 16227627]

11. de Bruijn DR, dos Santos NR, Thijssen J, Balemans M, Debernardi S, Linder B, Young BD, Geurts van Kessel A. The synovial sarcoma associated protein SYT interacts with the acute leukemia associated protein AF10. Oncogene 2001;20:3281–3289. [PubMed: 11423977]

12. Perani M, Ingram CJ, Cooper CS, Garrett MD, Goodwin GH. Conserved SNH domain of the proto-oncoprotein SYT interacts with components of the human chromatin remodelling complexes, while the QPGY repeat domain forms homo-oligomers. Oncogene 2003;22:8156–8167. [PubMed: 14603256]

13. Eid JE, Kung AL, Scully R, Livingston DM. p300 interacts with the nuclear proto-oncoprotein SYT as part of the active control of cell adhesion. Cell 2000;102:839–848. [PubMed: 11030627]

14. Ito T, Ouchida M, Ito S, Jitsumori Y, Morimoto Y, Ozaki T, Kawai A, Inoue H, Shimizu K. SYT, a partner of SYT–SSX oncoprotein in synovial sarcomas, interacts with mSin3A, a component of histone deacetylase complex. Lab Invest 2004;84:1484–1490. [PubMed: 15467731]

15. O'Brien LE, Jou TS, Pollack AL, Zhang Q, Hansen SH, Yurchenco P, Mostov KE. Rac1 orientes epithelial apical polarity through effects on basolateral laminin assembly. Nat Cell Biol 2001;3:831–838. [PubMed: 11533663]

16. Yu W, Datta A, Leroy P, O'Brien LE, Mak G, Jou TS, Matlin KS, Mostov KE, Zegers MM. Beta1-integrin orients epithelial polarity via Rac1 and laminin. Mol Biol Cell 2005;16:433–445. [PubMed: 15574881]

17. Cowley BD Jr, Smardo FL Jr, Grantham JJ, Calvet JP. Elevated c-myc protooncogene expression in autosomal recessive polycystic kidney disease. Proc Natl Acad Sci USA 1987;84:8394–8398. [PubMed: 3479800]

18. Carone FA, Makino H, Kanwar YS. Basement membrane antigens in renal polycystic disease. Am J Pathol 1988;130:466–471. [PubMed: 3279792]

19. Debnath J, Muthuswamy SK, Brugge JS. Morphogenesis and oncogenesis of MCF-10A mammary epithelial acini grown in three-dimensional basement membrane cultures. Methods 2003;30:256–268. [PubMed: 12798140]

20. Debnath J, Brugge JS. Modelling glandular epithelial cancers in three-dimensional cultures. Nat Rev Cancer 2005;5:675–688. [PubMed: 16148884]

21. Simmons NL. Stimulation of Cl⁻ secretion by exogenous ATP in cultured MDCK epithelial monolayers. Biochim Biophys Acta 1981;646:231–242. [PubMed: 7295715]

22. Post SR, Rump LC, Zambon A, Hughes RJ, Buda MD, Jacobson JP, Kao CC, Insel PA. ATP activates cAMP production via multiple purinergic receptors in MDCK-D1 epithelial cells. Blockade of an autocrine/paracrine pathway to define receptor preference of an agonist. J Biol Chem 1998;273:23093–23097. [PubMed: 9722536]

23. Turner CM, King BF, Srai KS, Unwin RJ. Antagonism of endogenous putative P2Y receptors reduces the growth of MDCK-derived cysts cultured in vitro. Am J Physiol Renal Physiol 2006;292:15–25.

24. Wilson PD, Hovater JS, Casey CC, Fortenberry JA, Schweibert EM. ATP release mechanisms in primary cultures of epithelia derived from the cysts of polycystic kidneys. J Am Soc Nephrol 1999;10:218–229. [PubMed: 10215320]

25. Pretto D, Barco R, Rivera J, Neel N, Gustavson MD, Eid JE. The synovial sarcoma translocation protein SYT-SSX2 recruits beta-catenin to the nucleus and associates with it in an active complex. Oncogene 2006;25:3661–3669. [PubMed: 16462762]

26. Taylor AL, Kudlow BA, Marrs KL, Gruenert DC, Guggino WB, Schwiebert EM. Bioluminescent detection of ATP release mechanisms in epithelia. Am J Physiol 1998;275:1391–1406.

27. Elbashir SM, Harborth J, Lendeckel W, Yalcin A, Weber K, Tuschl T. Duplexes of 21-nucleotide RNAs mediate RNA interference in cultured mammalian cells. Nature 2001;411:494–498. [PubMed: 11373684]

28. Yu W, Fang X, Ewald A, Wong K, Hunt CA, Werb Z, Matthay MA, Mostov K. Formation of cysts by alveolar type II cells in three-dimensional culture reveals a novel mechanism for epithelial morphogenesis. Mol Biol Cell 2007;18:1693–1700. [PubMed: 17332496]

29. Liu KD, Datta A, Yu W, Brakeman PR, Jou TS, Matthay MA, Mostov KE. Rac1 is required for reorientation of polarity and lumen formation through a PI 3- kinase-dependent pathway. Am J Physiol Renal Physiol 2007;293:1633–1640.

30. Harden TK, Boyer JL, Nicholas RA. P2-purinergic receptors: subtype-associated signaling responses and structure. Annu Rev Pharmacol Toxicol 1995;35:541–579. [PubMed: 7598506]

31. Erb L, Liao Z, Seye CI, Weisman GA. P2 receptors: intracellular signaling. Eur J Physiol 2006;452:552–562.

32. Insel PA, Ostrom RS, Zambon AC, Hughes RJ, Balboa MA, Shehnaz D, Gregorian C, Torres B, Firestein BL, Xing M, Post SR. P2Y receptors of MDCK cells: epithelial cell regulation by extracellular nucleotides. Clin Exp Pharmacol Physiol 2001;28:351–354. [PubMed: 11339212]

33. Braunstein GM, Roman RM, Clancy JP, Kudlow BA, Taylor AL, Shylonsky VG, Jovov B, Peter K, Jilling T, Ismailov I, Benos DJ, Scwiebert LM, Fitz JG, Schwiebert EM. Cystic fibrosis transmembrane conductance regulator facilitates ATP release by stimulating a separate ATP release channel for autocrine control of cell volume regulation. J Biol Chem 2001;276:6621–6630. [PubMed: 11110786]

34. Communi D, Janssens R, Suarez-Huerta N, Robaye B, Boeynaems JM. Advances in signalling by extracellular nucleotides. the role and transduction mechanisms of P2Y receptors. Cell Signal 2000;12:351–60. [PubMed: 10889463]

35. Schwiebert EM, Kishore BK. Extracellular nucleotide signaling along the renal epithelium. Am J Physiol Renal Physiol 2001;280:945–963.

36. Schwiebert EM, Zsembery A. Extracellular ATP as a signaling molecule for epithelial cells. Biochim Biophys Acta 2003;1615:7–32. [PubMed: 12948585]
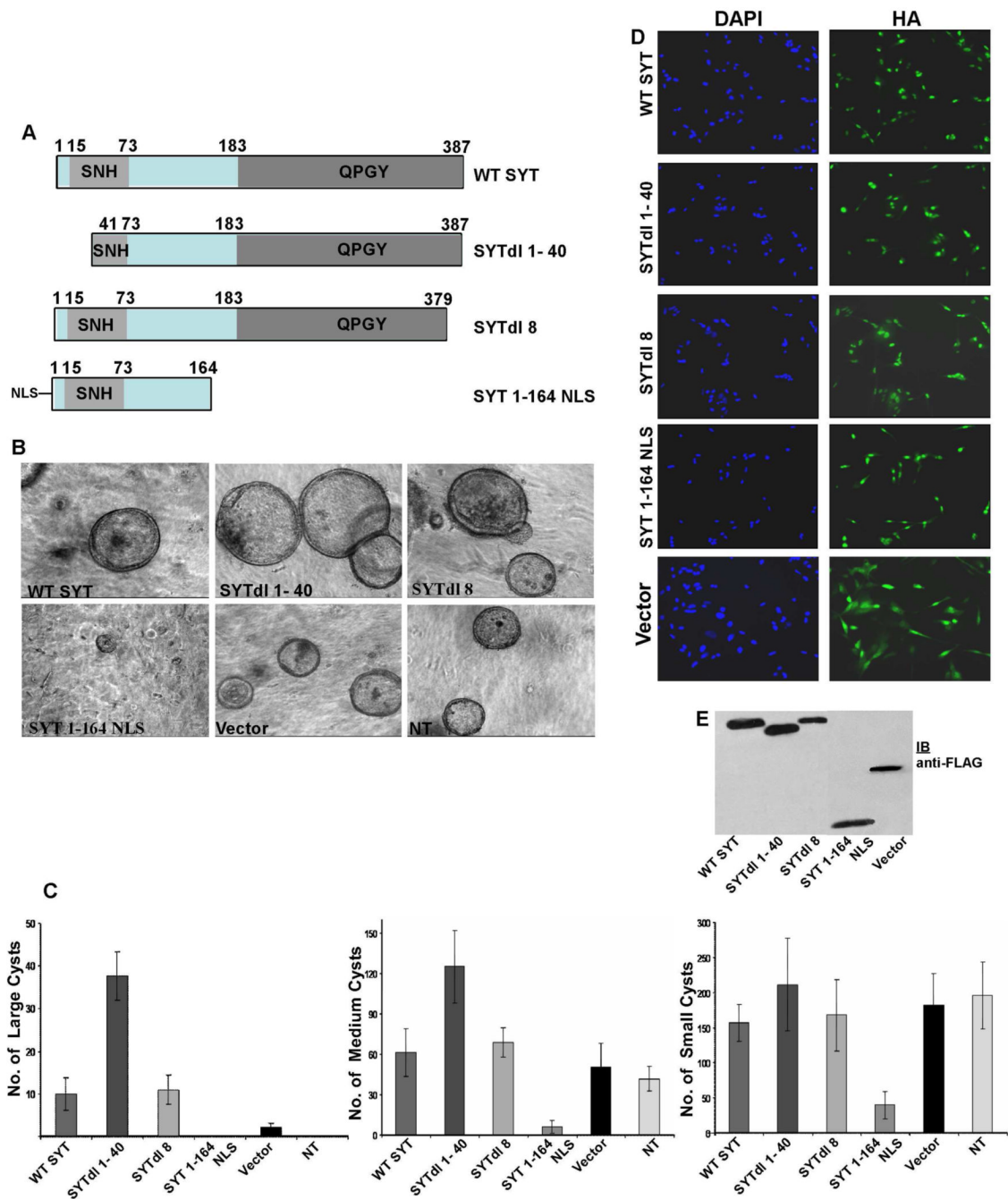
Fig.1. Effect of SYT domain expression on the growth of MDCK cysts
(**A**) Schematic representation of wild type SYT (WT SYT; 1–387 aa) and its mutants including the SYT functional domains QPGY and SNH. (**B**) 3D collagen cultures of MDCK cells expressing Flag/HA- tagged pOZ vector, WT SYT, SYTdl 1–40, SYTdl 8 and SYT 1–164NLS. NT: not-transfected. (**C**) Data analysis of the relative number and size of MDCK cysts expressing the various SYT-derived cDNAs. Large is >250 μm diameter, Medium is 150–250 μm diameter and Small is <150 μm in diameter. The data shown are representative of four independent experiments (n=4). (**D**) Infection efficiency of the pOZ retroviral transduction system. MDCK cells were infected with FLAG/HA tagged pOZ retroviral vector expressing WT SYT, SYTdl 1–40, SYTdl 8 and SYT 1–164NLS. HA- specific antibody was used for

visualization of the expressed proteins. The cytoplasmic HA staining in pOZ vector infected cells is due to the generation of an irrelevant FLAG/HA-tagged peptide by the vector. Magnification 20X. **(E)** Expression levels of the pOZ proteins in MDCK cells visualized with the Flag antibody. **The protein band in the pOZ vector lane is the irrelevant vector-generated polypeptide that disappears upon subcloning of SYT cDNAs.**
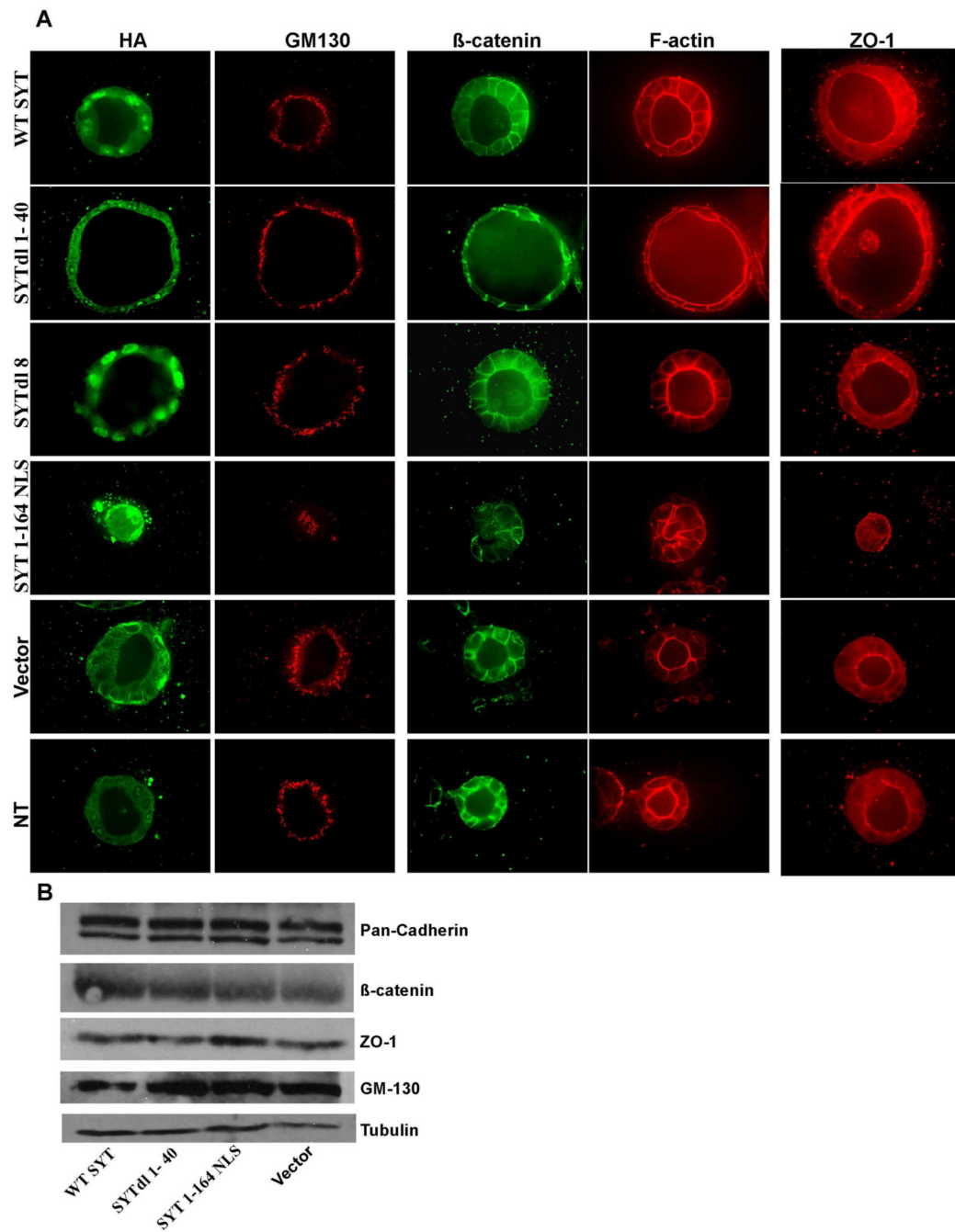
Fig. 2. Integrity of epithelial polarity in SYT expressants
Confocal microscopy of MDCK cells infected with WT SYT, the SYT deletion (dl) mutants, and grown in collagen for 7 days. **(A)** Cysts were double stained with antibodies to the apical Golgi protein GM130 (red) and with anti-HA antibody (to visualize the expressed SYT cDNAs). Polarization was also assessed by the luminal localization of an actin ring (red) at the apical surface, the basolateral marker β-catenin (green) and the apical marker ZO-1 (red). **(B)** Cellular levels of polarity markers in the monolayers of SYT dl mutants-expressing MDCK cells.
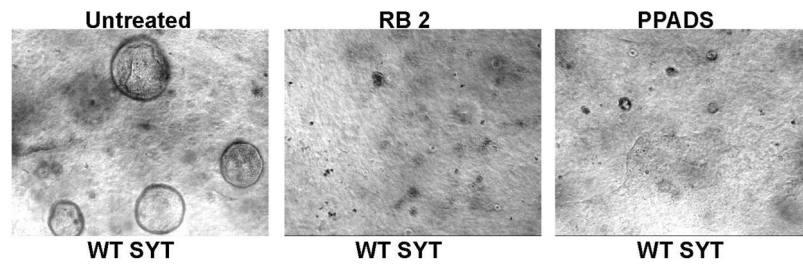
Fig. 3. Inhibition of SYT-MDCK cyst formation by the P2Y inhibitors
Left image: untreated cells. Center image: inhibition of cystogenesis by reactive blue 2. Right image: inhibition of cystogenesis by PPADS. Images represent bright field microscopy with 10X magnification.
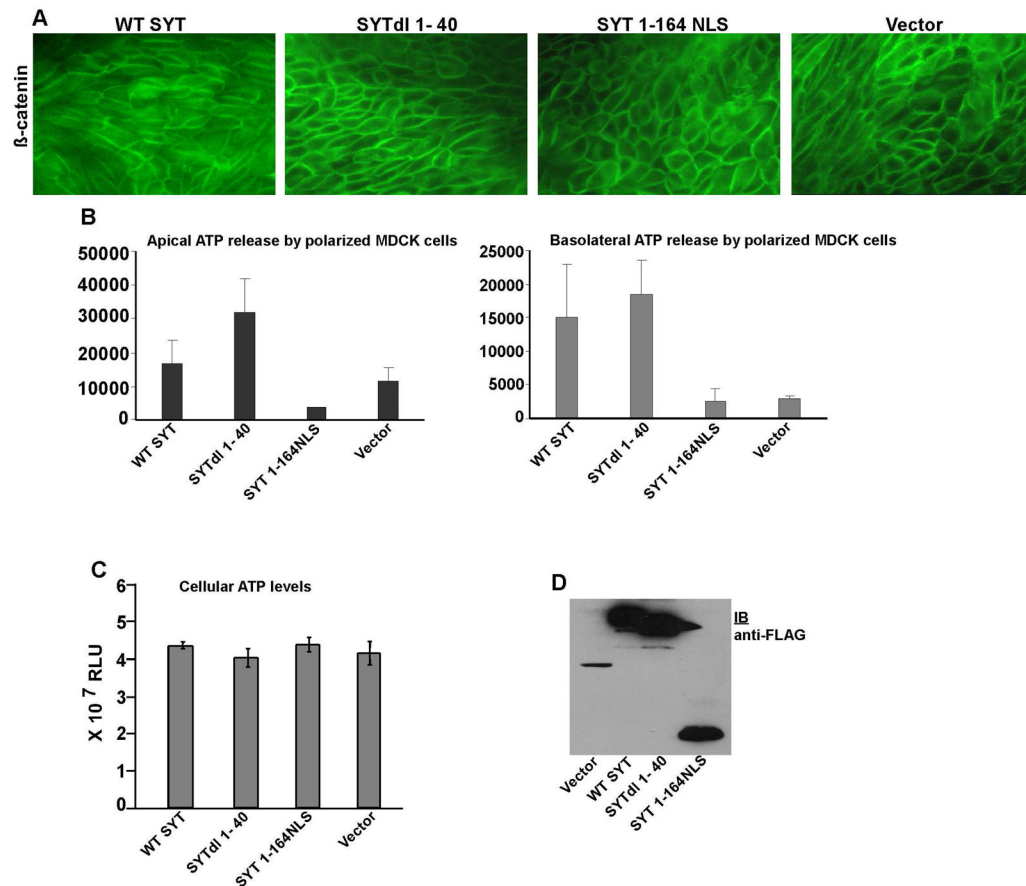
Fig. 4. Effect of SYT mutants on apical and basolateral ATP release by polarized MDCK cells
(A) Immunostaining of β-catenin in polarized MDCK cells expressing WT SYT and SYT dl mutants. **(B)** ATP released from apical and basolateral surfaces of MDCK cells expressing WT SYT and various SYTdl mutants. The values were recorded as Relative Light Units (RLU). **(C)** Steady state levels of intracellular ATP produced in control vector-, WT SYT-, SYTdl 1–40-, and SYT 1–164NLS-polarized MDCK cells. Measurements were reproduced in 3 independent experiments (n=3), each conducted in triplicates. **(D)** Expression levels of WT SYT, SYTdl1–40, and SYT1-164NLS in polarized MDCK cells visualized with the anti-FLAG antibody. The protein band in the pOZ vector-lane is the irrelevant vector-generated polypeptide that disappears upon subcloning of SYT cDNAs.
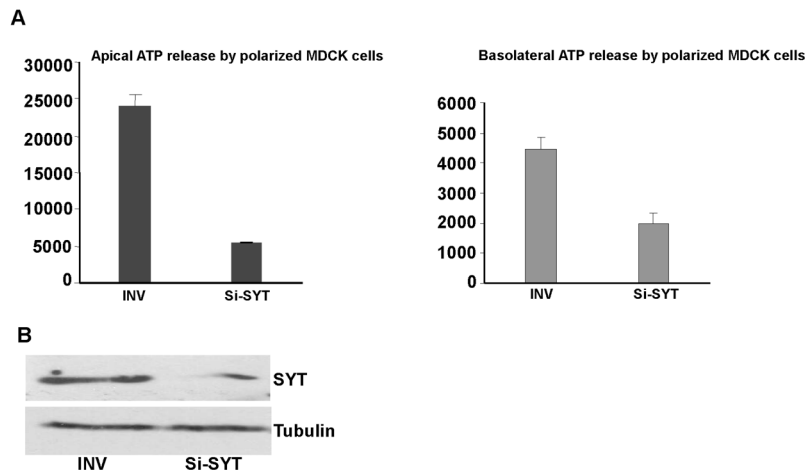
A

B

Fig. 5. Effect of SYT depletion on apical and basolateral ATP release by polarized MDCK cells
(A) MDCK cells were transfected with Si-SYT (SYT-specific) or control (INV) RNA oligomers. Measurements were reproduced in 3 independent experiments (n=3), each conducted in triplicates. **(B)** Specific depletion of cellular SYT by Si-SYT in MDCK cells. Alpha-tubulin (α) was used as loading control.
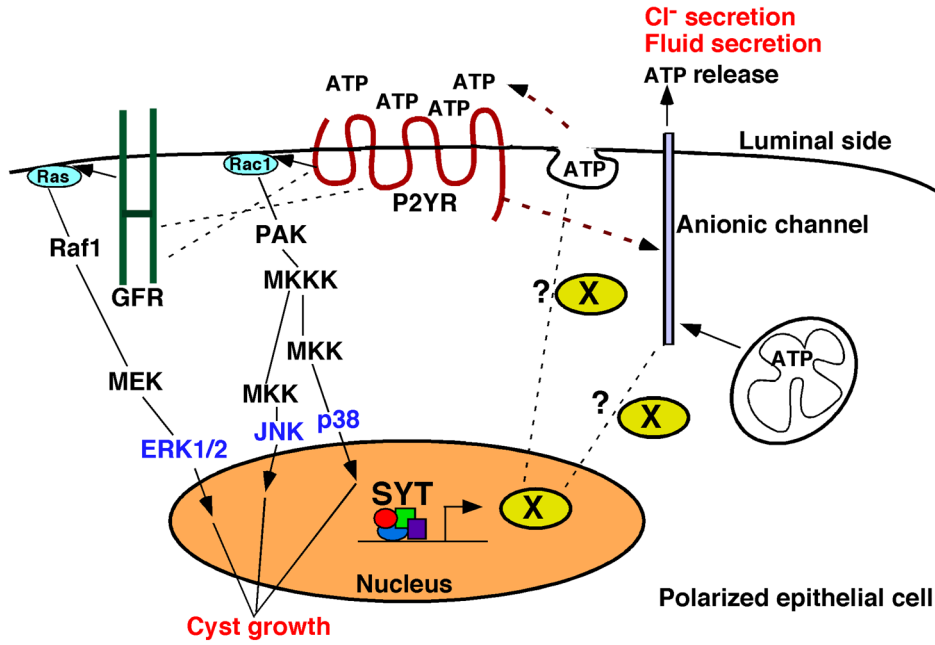
Fig. 6. A putative model for stimulation of MDCK cyst growth by SYT
SYT induces the expression of a positive modulator for ATP release in the polarized cell. ATP release in the luminal space could occur through ionic channels or vesicular transport [36]. Once released, ATP activates P2Y receptors that stimulate ion channels capable of transporting Cl⁻ and ATP to the extracellular space and osmotically drive fluid in the cyst lumen. Active P2Y receptors exert a proliferative effect on the lining polarized cells through Rac1-MAPK signaling or cross-talk with mitogenic growth factor receptors.

Table 1

Effect of signaling inhibitors on MDCK cyst formation

			Effect on cyst formation	
Inhibitor	**Conc.(µM)**	**Pathway affected**	**WT SYT**	**SYTdl 1–40**
Untreated	-----	-----	None	None
DMSO	-----	-----	None	None
Genestein	40	Tyrosine kinase CFTR	Complete inhibition	Complete inhibition
AG1478	10	EGFR	None	None
Reactive Blue 2	500	P2YR	Complete inhibition	Complete inhibition
PPADS	500	P2YR	Profound inhibition[†]	Profound inhibition
NF023	50	P2XR	None	None
LY290042	10	PI3K	Reduced Growth[a]	Reduced Growth
H-89	10	PKA	None	None
Calphostin	2.5	PKC	None	None
W-7	50	Calcium	None	None
PD98069	50	MEK1	Complete inhibition	Complete inhibition
SP600125	50	JNK	Complete inhibition	Complete inhibition
SB220025	50	p38MAPK	Complete inhibition	Complete inhibition
Rac Inhibitor	50	Rac1	Complete inhibition	Complete inhibition

[a] reduced growth signifies that the size of the individual MDCK cysts was around half the size of the untreated control. **Bolded names designate P2YR specific inhibitors.**

[†] Profound inhibition implies a very significant reduction in the number of intact cysts caused by the PPADS inhibitor. The reduction is quantitated in Table 2.

Table 2

Effect of P2Y inhibitors on MDCK cyst formation

	Untreated		RB 2 (500 uM)		PPADS (500 uM)	
	total cysts[*]		total cysts	%[†]	total cysts	%
POZ vector	98, **87**		0, **0**	0, **0**	2, **7**	2, **8**
WT SYT	277, **252**		0, **0**	0, **0**	36, **58**	13, **23**
SYTdl 1–40	287, **279**		0, **0**	0, **0**	115, **67**	40, **24**

[*] Total number of intact cysts contained in a well/collagen culture. Unbolded are numbers of cysts obtained in Experiment #1 and **bolded numbers are those of Experiment #2**

[†] % numbers represent the ratio of total number of intact cysts in each treated well over total number of intact cysts in an untreated well. Unbolded numbers are derived from Experiment #1 and **bolded numbers Are those of Experiment #2**